

Studies of exotic light nuclei with nucleon transfer reactions

A.H. Wuosmaa

Physics Department, Western Michigan University,
Kalamazoo, MI 49008-5252, U.S.A.

Recibido el 3 de enero de 2006; aceptado el 4 de abril de 2006

For decades, single nucleon transfer reactions such as (d, p) have served as fundamental tools for studying the properties of nuclei throughout the periodic table. Their selectivity and ease of interpretation have made them some of the most heavily used reactions for the determination of quantum numbers, and for probing the wave functions of single-particle states in nuclei. With the advent of radioactive beams, interest in these simple transfer reactions has been renewed. I will review the utility of such reactions, and discuss some current applications in the context of the modern theoretical understanding of nuclear structure and in nuclear astrophysics. Finally, I will discuss two recent examples of studies of the (d, p) reaction carried out with radioactive beams to study the light nuclei ^9Li and ^7He , and present some of the challenges and opportunities that await in this new domain.

Keywords: Nucleon transfer reactions; spectroscopic factors; radioactive beams.

Reacciones de transferencia de un nucleón han funcionado por décadas como herramientas fundamentales para estudiar las propiedades nucleares. Por su selectividad y fácil interpretación dichas reacciones han sido las más usadas en la determinación de los números cuánticos y como prueba de las funciones de onda de los estados de partícula independiente. La disponibilidad de haces radioactivos ha causado un interés renovado en esas reacciones de transferencia. Se revisan y se discuten algunas aplicaciones recientes de esas reacciones en la estructura nuclear y la astrofísica nuclear. Finalmente, se estudia la reacción (d, p) llevada a cabo con haces radioactivos para investigar los núcleos ligeros ^9Li y ^7He , y se presentan algunos retos y oportunidades para el futuro.

Descriptores: Reacciones de transferencia de nucleones; factores espectroscópicos; haces radioactivos.

PACS: 21.10.Jx; 25.60.Je; 21.10.Hw; 27.20.+n

1. Introduction

Single nucleon transfer reactions have, for many decades, played a major role in the development of the understanding of the structure of nuclei. Reactions such as (d, p) have served as fundamental tools for studying the properties of single-particle states in nuclei throughout the periodic table. The selectivity and ease of interpretation of the (d, p) reaction in particular have made it one of the most heavily used reactions for the determination of quantum numbers, and for probing the wave functions of single-particle states in nuclei. The question is, can we, after some 50 years of studying (d, p) reactions and others like it, still hope to learn new physics from such “classical” nucleon transfer reactions?

With the advent of radioactive beams, the answer to this question is emphatically yes. Interest in direct transfer reactions such as (d, p) has been renewed and invigorated with the possibility to test new, powerful theoretical methods for calculating nuclear structure, as well as the ability to address new questions in nuclear astrophysics. Modern, so-called *ab-initio* methods for calculating nuclear structure including the Quantum Monte Carlo (QMC) [1] and No-Core Shell Model [2] techniques have had considerable success in reproducing many properties of light nuclei with $A \leq 12$. In many light nuclei far from stability, however, few data are available with which to test these methods. With unstable beams, however, many such nuclei away from stability are now within reach. These reactions have also been employed in heavier, neutron-rich nuclei in the search for modifications to shell structure as compared to stable nuclei [3].

Two examples of nuclei for which data are limited are ^9Li and ^7He . Both are *p*-shell nuclei whose properties can be calculated within the frameworks of these modern theoretical methods. Calculations of spectroscopic factors for neutron transfer constitute a sensitive probe of the nuclear wave function, and can be calculated using these techniques [4, 5]. In ^7He , considerable uncertainty remains regarding the nature of the first excited state, while many theoretical results are in general agreement [1, 2, 6–8], reports of experimental work in the literature are contradictory [9–15]. Further knowledge about this nucleus, and other light very neutron-rich systems can help us to probe the range of applicability of these new theoretical methods. In particular, it is unclear whether these techniques in their present form can be applied to broad unbound states lying high in the continuum. Population of such short-lived resonances by simple, direct-transfer reactions opens a new window for detailed study of these loosely bound, or unbound systems.

Table I lists some calculated and experimental properties for states in the nuclei ^9Li and ^7He . The theoretical excitation energies from the Green’s Function Monte Carlo [1] and NCSM [2] are listed. For ^9Li , the theoretical spectroscopic factors are obtained using the Variational Monte Carlo (VMC) technique that provides the starting point for the GFMC calculations. Details on the calculation of the VMC spectroscopic factors are given in Ref. 4. Experimental results are from [4, 16].

TABLE I. Theoretical excitation energies and spectroscopic factors for ${}^9\text{Li}({}^8\text{Li}_{g.s.} + n)$ and ${}^7\text{He}({}^6\text{He}_{g.s.} + n)$ from [1,2,4,5], and experimental spectroscopic factors from [4, 16]. “S(Total)” corresponds to the calculated or measured spectroscopic factor from neutron transfer, and “S(Γ)” is the value determined from an R-matrix analysis of the widths of the unbound states where known, taken from the literature.

Nucleus	J^π	Theory			Experiment			
		E_X (MeV) GFMC	E_X (MeV) NCSM	S(Total) VMC	S(Total) NCSM	E_X (MeV)	S(Total) (d, p)	S(Γ)
${}^9\text{Li}$	$3/2^-$	0.0	0.0	1.11	1.05	0.00	0.90(13)	—
	$1/2^-$	1.5(4)	1.53	0.52	0.52	2.691	0.73(15)	—
	$5/2^-$	3.0(4)	4.54	0.78	0.84	4.31	0.93(20)	0.55(30)
	$3/2^-$	3.6(5)	5.52	0.42	0.21	5.38	—	—
	$7/2^-$	5.7(4)	6.71	0.009	0.002	6.43	—	—
${}^7\text{He}$	$3/2^-$	0.0	0.0	0.53	—	0.00	0.37(7)	0.31(6)
	$1/2^-$	2.9(3)	2.3	0.87	—	(2.6)	—	—
	$5/2^-$	3.3(2)	3.7	—	—	—	—	—
	$3/2^-$	3.8(2)	4.4	—	—	—	—	—

Also, data for neutron transfer in light nuclei may be useful for understanding some aspects of (n, γ) capture reactions which may be relevant to both non-standard big-bang nucleosynthesis and the early stages of the r process [18]. As the nuclei of interest are unstable, neutron capture cannot be studied directly in the conventional way, and so indirect methods must be applied. The (d, p) reaction provides one way to access this important information.

Such measurements present new experimental difficulties, however. For the (d, p) reaction, the most important information comes from the measurement of proton angular distributions at forward angles in the center-of-mass system. With radioactive beams, the experiments must be carried out in an inverse-kinematic regime, with the protons of interest being detected at backward angles in the laboratory. There, the protons have low energies and due to the kinematics of the reaction the separation in laboratory energy between groups of protons coming from different excited states becomes small, and energy as well as laboratory angle resolution becomes critical. Also, the solid-angle transformation between laboratory and center of mass is unfavorable, and large laboratory angle ranges must be covered to obtain the needed sensitivity. Compounding these problems are the difficulties which accompany any measurement carried out with unstable beams, namely low beam intensities, potential impurities in the beam, and poor emittance characteristics.

2. Experiment

The experiments were carried out using radioactive beams of ${}^8\text{Li}$ and ${}^6\text{He}$ produced at the Argonne National Laboratory In-Flight production facility [19]. This facility produces secondary beams of unstable nuclei by bombarding a cryogenically cooled gas cell filled with either hydrogen or deuterium with an intense primary beam, and then collecting the heavy products of nucleon transfer (*e.g.* (d, p)) or charge-

exchange (*e.g.* (p, n)) reactions using a 6 T superconducting magnetic solenoid. The secondary particles of interest are separated from the primary beam using a combination of a bending magnet and collimating slits. In the cases discussed here, the primary beam was ${}^7\text{Li}$ at 81 MeV with an intensity of 45 pA. The gas cell was filled with D₂ kept at a pressure between 1000 and 1250 mbar. The secondary ${}^8\text{Li}$ and ${}^6\text{He}$ beams were produced with the ${}^2\text{H}({}^7\text{Li}, p){}^8\text{Li}$, and ${}^2\text{H}({}^7\text{Li}, {}^3\text{He}){}^6\text{He}$ reactions, respectively, with intensities of approximately 50000 and 10000 particles per second incident on target. The energies of the ${}^8\text{Li}$ and ${}^6\text{He}$ beams were 76 and 69 MeV, respectively.

Figure 1 illustrates a schematic diagram of the experimental setup. The ${}^8\text{Li}$ and ${}^6\text{He}$ particles were incident on a $(\text{CD}_2)_n$ foil of areal density 540 $\mu\text{g}/\text{cm}^2$. The protons emitted towards backward angles (forward proton angles in the center-of-mass system) were detected in a set of three annular segmented silicon detectors which recorded their position and energy. The laboratory segmentation of the annular detectors was approximately 1°. Heavy beam-like fragments, including ${}^{7,8,9}\text{Li}$, or ${}^{4,6}\text{He}$ ions were detected and identified in a set of silicon ΔE - E telescopes covering $1^\circ < \theta_{\text{lab}} < 7^\circ$. To determine the total number of incident ions, and to

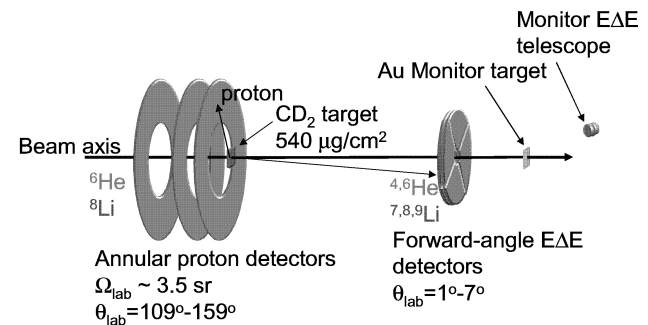


FIGURE 1. Schematic diagram of the experimental setup.

monitor the quality of the beam, beyond the ΔE - E array the beam particles scattered from a gold foil were detected in a second ΔE - E telescope. In addition, a fraction of singles events in the large ΔE - E array was recorded so as to monitor the beam scattering from the carbon nuclei in the $(CD_2)_n$ foil. The Q-value resolution of the setup (≈ 350 keV) was dominated by the beam-spot size (5×5 mm) and the segmentation of the silicon detector array. The experimental setup is described in detail in Ref. 4.

Figure 2 shows data obtained using the forward-angle telescope moved to 0° demonstrating the purity and quality of the beams that can be obtained. For these two beams, due to the large difference in mass-to-charge ratio m/q , primary-beam impurities on target were almost completely eliminated. Figure 2a shows an example of a particle identification spectrum at 0° for the ^8Li beam, illustrating only small amounts of impurities that have no effect on the measurement. Figure 2b shows an energy spectrum for the beam from an earlier run at slightly lower energy, which is quite narrow due to the limited straggling of the light Li ions in the foils of the secondary-beam production target. For calibration purposes and for verifying the efficiency of the setup, data were also obtained with the ^7Li primary beam after it was degraded in the secondary-beam production cell.

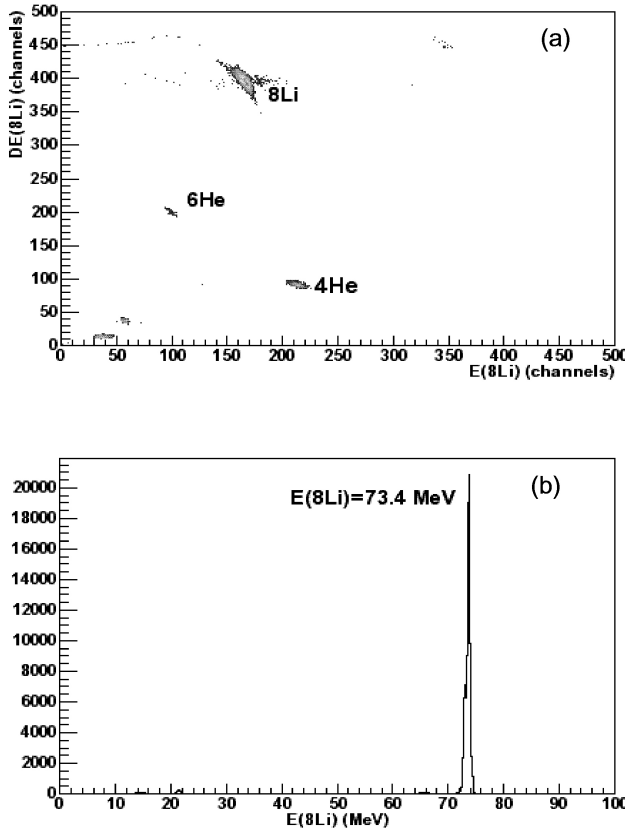


FIGURE 2. (a) Particle identification spectrum for secondary ^8Li beam. (b) Energy spectrum of secondary ^8Li beam.

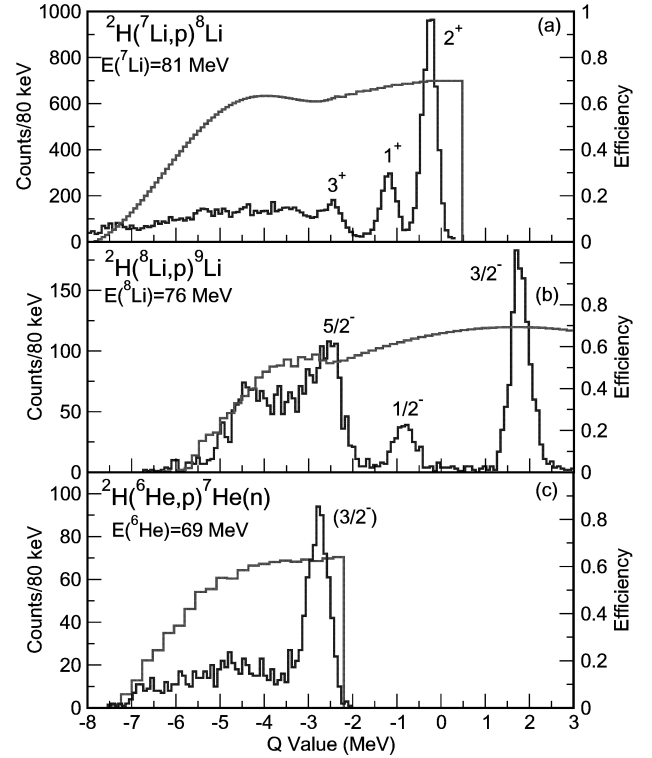


FIGURE 3. (a) Q-value spectrum for the $^2\text{H}(^7\text{Li},p)^8\text{Li}$ reaction from $p-^{7,8}\text{Li}$ coincidence events. (b) Q-value spectrum for the $^2\text{H}(^6\text{He},p)^7\text{He}$ reaction from $p-^6\text{He}$ coincidence events. In both cases the data are taken over the entire angular range covered by the proton detectors ($\theta_{lab} = 109$ to 159°). The histograms represent the Q-value dependence of the total detection efficiency.

3. Results

Q-value spectra for the $^2\text{H}(^7\text{Li},p)^8\text{Li}$, $^2\text{H}(^8\text{Li},p)^9\text{Li}$ and $^2\text{H}(^6\text{He},p)^7\text{He}$ reactions are shown in Fig. 3. The events represent protons in coincidence with identified $^{7,8,9}\text{Li}$ for the Li induced reactions, or ^6He particles for $^2\text{H}(^6\text{He},p)^7\text{He}$. The total detection efficiency of the setup in each case is given by the red histogram, and is obtained from a Monte-Carlo simulation that includes realistic detector geometries, and when appropriate the 3-body final states for excitation energies above the neutron binding energy in each case. For $^2\text{H}(^8\text{Li},p)^9\text{Li}$, the ground, first- and second-excited states are clearly observed. Some structure near $Q=-4.5$ MeV may correspond to the 6.4 MeV excited state, however this region is close to the detector energy threshold. For $^2\text{H}(^6\text{He},p)^7\text{He}$, the ground state is populated clearly and strongly, and at higher excitation energies there appears a broad distribution of counts in the excitation-energy range expected for a $1/2^-$ first-excited state as predicted by a variety of theoretical calculations. Little evidence for a low-lying first excited state near 600 keV as was reported in Ref. 12 is observed in the data for the $^2\text{H}(^6\text{He},p)^7\text{He}$ reaction.

Figure 3 shows angular distribution data for the (a) $^2\text{H}(^8\text{Li},p)^9\text{Li}$ and (b) $^2\text{H}(^6\text{He},p)^7\text{He}$ reactions. For $^2\text{H}(^8\text{Li},p)^9\text{Li}$, the data are plotted with curves calculated

using the DWBA program PTOLEMY [20], using spectroscopic factors from the Variational Monte Carlo (VMC) calculations as described in Refs 1 to 4 and given in Table I. The solid and dashed curves represent the predictions obtained using two different optical-model potential sets taken from Ref. 21. The curves represent absolute predictions of the angular distribution with no further normalization and are in good agreement with the data. Table 1 also lists the deduced experimental neutron spectroscopic factors taken from the comparison between theory and experiment. For the ground state of ${}^7\text{He}$, the shape of the measured angular distribution is well described by the PTOLEMY calculation (solid line), however the magnitude is slightly lower, suggesting an experimental ${}^6\text{He}_{g.s.} + n$ spectroscopic factor approximately 0.69 times smaller than the calculated one, or $S({}^6\text{He}_{g.s.} + n) = 0.37 \pm 0.07$. The diamond symbols and dashed line represent the results extracted for a possible excited state in ${}^7\text{He}$ as described below. For comparison, Table I also lists the values of the spectroscopic factors obtained from an R-Matrix analysis of the widths of the unbound states as quoted in the literature [22].

To address the question of possible excited states of ${}^7\text{He}$, the ${}^2\text{H}({}^6\text{He},p){}^7\text{He}$ Q-value spectrum, corrected for detection efficiency, appears in Fig. 5a. To reproduce the spectrum, we generated simulated spectra for the ground state, and a set of hypothetical broad states whose line shapes were obtained from the R-Matrix formalism with modifications from the dependence of the cross section on Q value from the

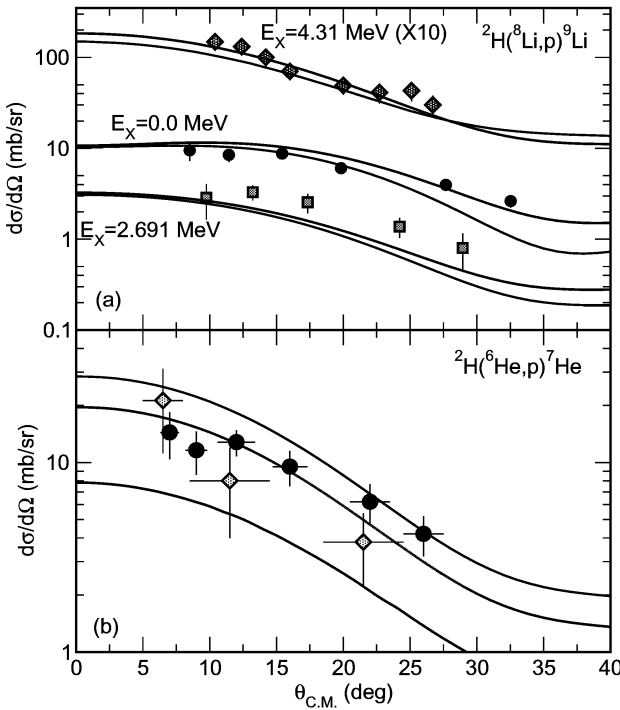


FIGURE 4. (a) Proton angular distributions for the ground, first- and second-excited states in ${}^9\text{Li}$ from ${}^2\text{H}({}^8\text{Li},p){}^8\text{Li}$. The curves are described in the text. (b) Angular distribution for ${}^2\text{H}({}^6\text{He},p){}^7\text{He}$ ground state (filled circles) and excited state (diamonds). Curves are described in the text.

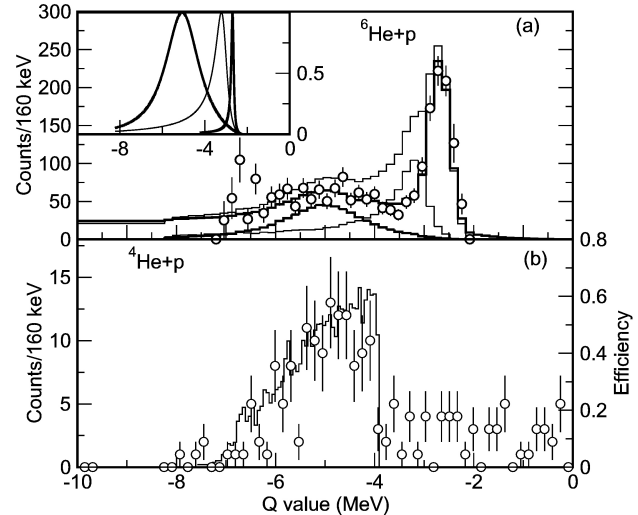


FIGURE 5. (a) Q-value spectrum for the ${}^2\text{H}({}^6\text{He},p){}^7\text{He}$ reaction from $p-{}^6\text{He}$ coincidence events corrected for detection efficiency. The histograms are described in the text. (Inset) Line shapes for different resonances used in the analysis of the efficiency-corrected Q-value spectrum. (b) Q-value spectrum for ${}^2\text{H}({}^6\text{He},p){}^6\text{He} \rightarrow {}^4\text{He} + n$.

PTOLEMY calculations described above. The data are best described by including the ground state, a broad excited state at $E_X=2.6$ MeV and width $\Gamma=2.0$ MeV, and also a smooth empirical background. The resonance line shapes included in the fit are shown in the insert to Fig. 5. The thin histogram in Fig. 5a illustrates a fit including contributions that well describe the data plus a contribution from the proposed low-lying first excited state described in Ref. 12 expected if it were populated with the theoretically anticipated spectroscopic factor. The data clearly do not support the presence of such a state populated with that magnitude in the (d,p) reaction. The extracted cross sections for a possible $1/2^-$ state from this analysis are given by the diamond symbols in Fig. 4. The corresponding calculated cross section for a $1/2^-$ state populated with the theoretical spectroscopic factor given in Table I is shown as the dashed line. The data are in rough agreement with the calculation but are consistently higher, perhaps suggesting that the situation at higher excitation energy is more complex than assumed in this simple model. It is also possible that the theoretical approach for determining the (d,p) yield may not be completely appropriate when dealing with very broad states high in the continuum.

Plotted in Fig. 5b are data taken from ${}^4\text{He}+p$ coincidences, where events for ${}^2\text{H}({}^6\text{He},p){}^7\text{He} \rightarrow {}^6\text{He}(2^+) + n$ might appear. The Monte-Carlo efficiency for the ${}^4\text{He}+p$ final state, given by the histogram in Fig. 5b, is of the same magnitude as that for ${}^6\text{He}+p$. The yield is small, with a constant background from interactions of the ${}^6\text{He}$ beam with the carbon in the target. The small yield suggests that if a broad excited state in ${}^7\text{He}$ is populated in ${}^2\text{H}({}^6\text{He},p){}^7\text{He}$, it does not possess a large ${}^6\text{He}(2^+)$ decay branch, consistent with the expectations for a first excited state with spin and parity $1/2^-$.

4. Discussion and Conclusions

The present results show that nucleon transfer reactions such as (d, p) performed in inverse kinematics with light radioactive beams can be an effective tool for probing the detailed structure of exotic light nuclei. For ${}^9\text{Li}$, the measured (d, p) angular distributions and spectroscopic factors are in good agreement with modern *ab-initio* calculations, confirming the suggested $1/2^-$ assignment for the first-excited state and suggesting $J^\pi=5/2^-$ for the second-excited state.

The results for ${}^9\text{Li}$ are also of interest in relation to nuclear astrophysics and the early stages of the *r*-process. Terasawa *et al.* have pointed out that in environments where the *r*-process is thought to take place, frequently the very high entropy that is present results in large numbers of free nucleons and alpha particles [17]. In this case, reactions involving light nuclei must also be considered in order to understand the production of precursors to the conventional *r*-process that leads to heavier nuclei. One important reaction sequence for the production of such seed nuclei for the *r*-process is ${}^4\text{He}(t, \gamma){}^7\text{Li}(n, \gamma){}^8\text{Li}(\alpha, n){}^{11}\text{B}$. Due to the Coulomb barrier the ${}^8\text{Li}(\alpha, n){}^{11}\text{B}$ reaction stands as a bottleneck, and ${}^8\text{Li}$ may be depleted by the neutron-capture reaction ${}^8\text{Li}(n, \gamma){}^9\text{Li}$ [17, 18]. As the neutron capture reaction cannot be studied directly, indirect methods may be used and, as described in Ref. 18 this quantity may be deduced from the cross section for ${}^8\text{Li}(d, p){}^9\text{Li}$. Li *et al.* have also measured the ground state transition for this reaction at lower bombarding energies and found a ground-state spectroscopic factor in agreement with our value. From these results, it appears that the afore-mentioned depletion of ${}^8\text{Li}$ may be important in this context.

In ${}^7\text{He}$, the results for the ground state are in general accord with theoretical expectations, again providing a verifica-

tion of the predictions of the QMC calculations. For possible excited states in ${}^7\text{He}$, no evidence is found for a low-lying $1/2^-$ first-excited state, although the data do possibly suggest a broad resonant state centered at $E_X=2.6$ MeV, within the range for a first-excited state predicted by several theories. While some uncertainties exist in the extraction of the cross section for this possible resonance, it seems that the cross section for this transition is larger than expected, possibly revealing a deficiency in either the optical model parameters used, or in the method of determining the spectroscopic overlaps for very broad unbound states. While the energy of this possible state is slightly lower than that observed for a broad state in ${}^7\text{He}$ populated in heavy-ion transfer [9] and neutron pickup [10], it is possible that different reaction mechanisms may populated different states, or that the coherence effects with direct breakup could influence the shape of the spectrum.

Acknowledgments

The author gratefully acknowledges the contributions of his collaborators from Argonne National Laboratory: K.E. Rehm, J.P. Greene, D.J. Henderson, R.V.F. Janssens, C.L. Jiang, E.F. Moore, R. C. Pardo, D. Peterson, S.C. Pieper, G. Savard, J.P. Schiffer, S. Sinha, X. Tang, and R.B. Wiringa; Northwestern University: R.E. Segel and L. Jisonna; and Hebrew University: M. Paul. This work was supported by the U.S. Department of Energy, Office of Nuclear Physics under contract numbers DE-FG02-04R41320 (WMU), W-31-109-ENG-38 (ANL), DE-FG02-98ER4106 (NU), and the Faculty Research and Creative Activities Fund, Western Michigan University.

1. S.C. Pieper, R.B. Wiringa, and J. Carlson, *Phys. Rev. C* **70** (2004) 054325.
2. P. Navrátil and B.R. Barrett, *Phys. Rev. C* **57** (1998) 3119.
3. A. Obertelli *et al.*, *Phys. Rev. C* **71** (2005) 024304.
4. A. H. Wuosmaa *et al.*, *Phys. Rev. Lett.* **94** (2005) 082502.
5. P. Navrátil, *Phys. Rev. C* **71** (2004) 054324.
6. A.A. Wolters, A.G.M. van Hees, and P.W.M. Glaudemans, *Phys. Rev. C* **42** (1990) 2062.
7. J. Wurzer and H.M. Hofmann, *Phys. Rev. C* **55** (1997) 688.
8. D. Halderson, *Phys. Rev. C* **70** (2004) 041603.
9. H.G. Bohlen *et al.*, *Phys. Rev. C* **64** (2001) 024312.
10. A. Korsheninnikov *et al.*, *Phys. Rev. Lett.* **82** (1999) 3581.
11. F. Skaza *et al.*, *Phys. Lett. B* **619** (2005) 82.
12. M. Meister *et al.*, *Phys. Rev. Lett.* **88** (2002) 102501.
13. D. Frekers, *Nucl. Phys. A* **731** (2004) 76.
14. G.V. Rogachev *et al.*, *Phys. Rev. Lett.* **92** (2004) 232502.
15. P. Boutachkov *et al.*, *Phys. Rev. Lett.* **95** (2005) 132502.
16. A.H. Wuosmaa *et al.*, *Phys. Rev. C* **72** (2005) 061301(R).
17. M. Terasawa *et al.*, *Ap. Journal* **572** (2001) 470.
18. Z. H. Li *et al.*, *Phys. Rev. C* **71** (2005) 052801R.
19. B. Harss *et al.*, *Rev. Sci. Instrum.* **71** (2000) 380.
20. M.H. Macfarlane and S.C. Pieper, *Argonne National Laboratory Report ANL-76-11, Rev. 1* (1978).
21. J.P. Schiffer *et al.*, *Phys. Rev.* **164** (1967) 1274.
22. D.R. Tilley *et al.*, *Nucl. Phys. A* **708** (2002) 3.